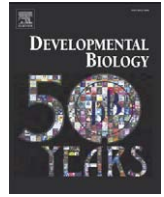




Contents lists available at ScienceDirect

Developmental Biology

journal homepage: [www.elsevier.com/developmentalbiology](http://www.elsevier.com/developmentalbiology)

## Three distinct RNA localization mechanisms contribute to oocyte polarity establishment in the cnidarian *Clytia hemisphaerica*

Aldine Amiel, Evelyn Houliston\*

Université Pierre et Marie Curie (Paris VI), Developmental Biology Unit, Observatoire Océanologique, 06230 Villefranche sur mer, France  
 Centre Nationale de la Recherche Scientifique UMR 7009, Observatoire Océanologique, 06230 Villefranche sur mer, France

### ARTICLE INFO

#### Article history:

Received for publication 30 June 2008  
 Revised 10 November 2008  
 Accepted 9 December 2008  
 Available online 16 December 2008

#### Keywords:

*Clytia*  
 Oogenesis  
 Meiotic maturation  
 Oocyte polarity  
 RNA localization  
 Frizzled  
 Wnt  
 Microtubule  
 Cnidaria

### ABSTRACT

Egg animal–vegetal polarity in cnidarians is less pronounced than in most bilaterian species, and its normal alignment with the future embryonic axis can be disturbed by low-speed centrifugation. We have analyzed the development of oocyte polarity within the transparent and autonomously functioning gonads of *Clytia* medusae, focusing on the localization of three recently identified maternal mRNAs coding for axis-directing Wnt pathway regulators. Animal–vegetal polarity was first detectable in oocytes committed to their final growth phase, as the oocyte nucleus (GV) became positioned at the future animal pole. In situ hybridization analyses showed that during this first, microtubule-dependent polarization event, CheFz1 RNA adopts a graded cytoplasmic distribution, most concentrated around the GV. CheFz3 and CheWnt3 RNAs adopt their polarized cortical localizations later, during meiotic maturation. Vegetal localization of CheFz3 RNA was found to require both microtubules and an intact gonad structure, while animal localization of CheWnt3 RNA was microtubule independent and oocyte autonomous. The cortical distribution of both these RNAs was sensitive to microfilament-disrupting drugs. Thus, three temporally and mechanistically distinct RNA localization pathways contribute to oocyte polarity in *Clytia*. Unlike the two cortical RNAs, CheFz1 RNA was displaced in fertilized eggs upon centrifugation, potentially explaining how this treatment re-specifies the embryonic axis.

© 2008 Elsevier Inc. All rights reserved.

### Introduction

In many animal species, a polarized distribution of “determinants” within the egg is crucial to direct normal development of the embryonic body plan. Localized or graded distributions of organelles and macromolecules commonly become established along the primary animal–vegetal (a–v) egg axis during oogenesis. The animal pole corresponds to the site of polar body emission during meiosis, and is often predicted by the position of the GV prior to meiotic maturation. The timing and mechanisms by which oocyte polarity is established have been well studied in classical models from the Bilateria, notably *Drosophila*, *Xenopus* and ascidians. In these cases, the decisive maternal localized determinants have been shown to consist of mRNAs positioned at different sites with respect to the a–v axis (Di Carlo, 2004; King et al., 2005; Nishida, 2005; van Eeden and St Johnston, 1999).

In the Cnidaria and Ctenophora, experimental evidence has indicated that pre-localized maternal factors may be less important for directing embryo organization than in the Bilateria (Freeman, 1976,

1981a). Thus in ctenophore embryos, the embryonic “oral” pole always forms at the site of first mitosis but does not necessarily relate to egg a–v polarity, as seen following physiological migration of the female nucleus away from the animal pole or experimental displacement of the zygote nucleus by centrifugation (Freeman, 1976, 1977; Houliston et al., 1993). Similarly in cnidarians, the single “oral–aboral” embryonic axis can be re-oriented from its usual alignment with the egg a–v axis by experimental displacement of the zygote nucleus (Freeman, 1981a). The sensitivity of embryonic axis specification to low-speed centrifugation in cnidarians and ctenophores distinguishes them from bilaterian models such as sea urchins, in which localized determinants are thought to be anchored tightly to the cortex of the egg along its a–v axis (Horstadius, 1953).

In cnidarians, despite the sensitivity of embryonic axis orientation to nuclear displacement, there is considerable evidence that in undisturbed eggs a–v polarity provides polarity cues for axial development. Firstly, the animal pole of the undisturbed egg has been shown to predict reliably the oral (=posterior) pole of the larva and the mouth end of the adult polyp in a number of cnidarians including the hydrozoans *Clytia* (=Phialidium), *Dynamena*, *Amphisbeta* and *Hydractinia*, and the anthozoan *Nematostella*, (Freeman, 1981a; Fritzenwanker et al., 2007; Lee et al., 2007; Teissier, 1931). Secondly, while many cnidarian oocytes and eggs appear visibly uniform, signs of polarity have been noted in some cases, including

\* Corresponding author. Université Pierre et Marie Curie (Paris VI), Developmental Biology Unit, Observatoire Océanologique, 06230 Villefranche sur mer, France. Fax: +33 4 93 76 37 92.

E-mail address: [houliston@obs-vlfr.fr](mailto:houliston@obs-vlfr.fr) (E. Houliston).

the eccentric position of the Germinal Vesicle (GV) at the animal pole, as well as polarized localization of pigment in *Amphisbetia* eggs and of symbiont dinoflagellates in the coral *Pocillopora* (Marlow and Martin-dale, 2007; Teissier, 1931). Thirdly, embryo manipulation studies in the hydrozoan *Podocoryne* and in *Nematostella* have provided experimental evidence for anally-localized axis-determining factors (Fritzenwanker et al., 2007; Lee et al., 2007; Momose and Schmid, 2006). In these two distantly-related cnidarians, bisection perpendicular to the a–v axis at the 8 cell-stage yields normal planula larva from the animal half but non-polarized ectodermal balls (lacking endodermal tissue) from the vegetal half, implying that determinants for both polarity and endoderm formation are excluded from the vegetal half of the early embryo. The formation of normally patterned larvae conserving the original polarity from animal fragments in these species, and from both animal and vegetal fragments in other species including *Clytia gregarium*, likely reflects the exceptional regulative ability of cnidarians at all stages of their life cycles (Freeman, 1981b; Galliot and Schmid, 2002).

Recent studies have shown that anally localized axis determinants in cnidarians act as regulators of the canonical Wnt signaling pathway, promoting stabilization and nuclear localization of the transcriptional co-factor  $\beta$  catenin on the future oral side of the early embryo (Momose and Houliston, 2007; Wikramanayake et al., 2003). Maternally directed Wnt pathway activation is thought to be an evolutionary ancient embryo patterning mechanism, functioning not only in cnidarians but also in many deuterostomes, including sea urchins, ascidians, amphibians and fish (Imai et al., 2000; Schneider et al., 1996; Wikramanayake et al., 1998) as well as in some protostomes (Henry et al., 2008). In *Clytia hemisphaerica* the localized maternal determinants upstream of Wnt pathway activation have been identified as mRNAs coding for two frizzled family receptor proteins, CheFz1 and CheFz3, found concentrated in the animal cytoplasm and at the vegetal cortex of the egg respectively (Momose and Houliston, 2007). CheFz1 mediates canonical Wnt pathway activation and directs the development of oral fate, while CheFz3 acts negatively to down-regulate this pathway in the future aboral territory. mRNA for the Wnt family ligand CheWnt3 is also maternally localized and essential for embryonic polarity development, exhibiting a third distinct localization pattern at the animal cortex (Momose et al., 2008). In other cnidarians, localized Wnt pathway activation may be directed by alternative or additional determinants: In *Nematostella*, no maternal RNA localization has been detected yet for Wnt ligands or receptors, but the cytoplasmic regulator protein Disheveled is localized maternally at the egg animal pole (Lee et al., 2007), while in *Hydractinia* maternal RNAs for both Wnt3 and the downstream transcription factor Tcf are localized (Plickert et al., 2006).

It is remarkable that unfertilized *Clytia* eggs, despite their lack of visible polarity, contain axis-directing mRNAs with three distinct distributions along the animal–vegetal axis: CheFz1 mRNA exhibiting a declining animal–vegetal gradient in the cytoplasm, CheWnt3 mRNA localized at the animal cortex and CheFz3 mRNA at the vegetal cortex. This provides an opportunity to examine the extent to which the cellular and molecular mechanisms responsible for generating egg and embryo polarity via mRNA localization are common between evolutionary distant phyla. Taking advantage of the exceptional transparency and developmental autonomy of the *Clytia* female gonad we have characterized by various techniques of microscopy the development of polarity during oocyte growth and during oocyte maturation, the light induced process that triggers meiosis completion and spawning of unfertilized eggs. Our study has defined distinct temporal characteristics and cytoskeletal requirements for the localization of each of these three key maternal mRNAs. We also performed centrifugation experiments to assess the anchoring of these localized RNAs in fertilized and unfertilized eggs, allowing us to address the basis of embryonic axis re-specification in *Clytia* upon nuclear displacement.

## Materials and methods

### *Medusae, gonads and oocytes*

*C. hemisphaerica* medusae were obtained from laboratory colonies (Chevalier et al., 2006). Oocytes and gonads were cultured in 0.2  $\mu$ m Millipore Filtered Sea Water (MFSW). Gonads were dissected from the underside of the bell of mature medusae using surgical scissors. Oocytes were liberated from dissected gonads by treatment with 1% Thioglycolate/0.05% Pronase/0.3 M NaCl for fixation, or without enzymatic treatment using fine forceps for maturation experiments. Maturation was triggered by incubation of dissected gonads or isolated fully-grown oocytes for 5–15 min in 2–4 mM bromo adenosine 3'5'cyclic MonoPhosphate (Br-cAMP) in MFSW, diluted just before use from a 20 mM aqueous stock, then washed in MFSW. All experiments were performed at 18–20 °C. We confirmed that Br-cAMP-matured *C. hemisphaerica* oocytes can fertilize and develop normally, as reported previously for *C. gregarium* (Freeman and Ridgway, 1988). Time-lapse recordings of oocyte maturation were made using DIC optics on a Zeiss Axiovert microscope equipped with a motorized stage and CCD camera driven by MetaMorph software.

### *Immunofluorescence*

For immunofluorescence, isolated gonads or oocytes were fixed and permeabilized in 0.1 M HEPES pH6.9/50 mM EGTA/10 mM MgSO<sub>4</sub>/0.5 M Maltose/4% paraformaldehyde (Methanol+RNase free/Electron Microscopy Science)/0.2% Triton X-100 for 2 h at room temperature, followed by washing in PBS/Triton X-100 0.2%. Microtubules were visualized by incubation in anti-tubulin antibody DM1A (Sigma diluted in 3% BSA/PBS) overnight at 4 °C, followed by a FITC coupled anti-mouse Ig (Sigma, diluted 1/500 in PBS) for 2 h at room temperature, with Hoechst dye 33258 (1  $\mu$ g/ml) included to stain DNA and rhodamine-phalloidin (1  $\mu$ g/ml; Sigma) to stain polymerized actin. PBS was used for washes between antibodies. Specimens were mounted in Citifluor (Citifluor Ltd) and imaged using a Leica SP2 confocal microscope.

### *In situ hybridization*

In situ hybridization was performed exactly as described previously (Chevalier et al., 2006) using DIG-labeled antisense RNA probes, synthesized from linearized Express1 plasmid using T7 or T6 or SP6 polymerase and the RNA DIG-labeling mix (Roche). Following in situ hybridization, each egg and oocyte was examined under the microscope and the distribution of the signal assessed in relation to the position of the nucleus, visualised using with Hoechst dye. Separate localization criteria were established for each RNA: CheFz1, which in normal unfertilized eggs shows a declining animal–vegetal gradient in the cytoplasm (Momose and Houliston, 2007), was considered to be localized if its concentration of the RNA signal was higher in the hemisphere containing the nucleus than in the opposite hemisphere. The two cortical RNAs were considered to be localized if the majority of the staining was located in the half of the cortex opposite (for CheFz3) or centered on (for CheWnt3) the nucleus. Note that when assessing RNA localization we took into consideration the natural variation in intensities and distributions of the in situ signal between eggs.

### *Cytoskeletal inhibitor treatments and centrifugation*

Dissected gonads, maturing oocytes and unfertilized eggs were treated with 10  $\mu$ M nocodazole to depolymerize microtubules, or 10  $\mu$ g/ml cytochalasin B or lantrunculin B to disrupt microfilaments, diluted into MFSW just before use from stock solutions in DMSO. Equivalent results were obtained using cytochalasin B and

lantrunculin B. Controls were incubated in MFSW containing equivalent concentrations of DMSO. For centrifugation, eggs pre-treated in some cases with 10  $\mu$ M nocodazole for 20 min, were suspended in 0.3% low melting temperature agarose/MFSW (maintained liquid at 25 °C until use) and centrifuged for 10 min at 800  $\times$ g at 4 °C. Fertilized eggs were centrifuged 25 min after gamete mixing. After centrifugation, eggs were liberated by warming to 60 °C for a few seconds, then washed 3 times in MFSW. This procedure was found to

displace the egg nucleus in fertilized eggs (Freeman, 1981a) and in unfertilized eggs treated with nocodazole, but not in untreated unfertilized eggs, which have a dense microtubule network surrounding the nucleus (see Figs. 7p–r).

**Results**

*Ordered progression of oocyte growth and polarization in the Clytia gonad*

To address the origin of the oocyte a–v polarity in *Clytia*, we first undertook a detailed characterization of growing oocytes in adult female medusae. The medusa is completely transparent, allowing direct examination of growing oocytes within the gonads, while the transparency of the yolk allows nuclei to be visualized clearly even in fully grown (160–180  $\mu$ m diameter) oocytes (Figs. 1a, b). Remarkably, isolated *Clytia* gonads cultured in filtered sea water undergo successive cycles of oocyte growth and ovulation for several days, responding normally to the light cues that induce spawning and maturation of competent oocytes (Honegger et al., 1980).

The gonads of sexually mature female *Clytia* medusae hang on the sub-umbrellar side of the bell from each of the four endodermal radial canals (Figs. 1a, c). The oocytes are arranged on each side of the endodermal cavity and are covered by a thin ectodermal epithelium, thus being sandwiched between layers of endoderm and ectoderm (Fig. 1c). Proliferating germ cell precursors and oocytes undergoing the first stages of meiosis lie close to the medusa bell. Growing oocytes showing yolk accumulation in the cytoplasm (vitellogenesis) are positioned more distally, although they do not necessarily show a strictly ordered size progression. Meiosis is arrested at the diplotene stage during vitellogenesis. In the smallest visible vitellogenic oocytes, the Germinal Vesicle (GV) is central and there are no apparent signs of cytoplasmic or cortical asymmetry. Fully-grown oocytes, however, are clearly polarized, with the GV consistently positioned on the ectoderm side, defining the future animal pole.

To understand the relationship between oocyte growth and polarization, we isolated vitellogenic oocytes from uniform medusa populations at successive times during the growth-spawning cycle, and classified them according to three principal stages of oocyte growth (Fig. 2; Table 1; results summarized in Fig. 1d). Stage I growing oocytes (less than 120  $\mu$ m in diameter) are characterized by a single, large nucleolus within a central GV (Figs. 2a, e). As has been described in related species (Faulkner, 1929; Hargitt, 1919), this characteristic large nucleolus fragments during the subsequent growth phase. Stage II oocytes (120–160  $\mu$ m diameter) are characterized by a fragmented nucleolus and semi-dispersed chromatin. During late stage II (oocytes 140–160  $\mu$ m in diameter), the nucleolus is completely fragmented and individual chromosomes become progressively more condensed, remaining close to the GV membrane (Fig. 2h). The GV first starts to reposition during the stage II period (see below). In stage III oocytes (160–180  $\mu$ m in diameter) the GV is close to the surface, nucleoli

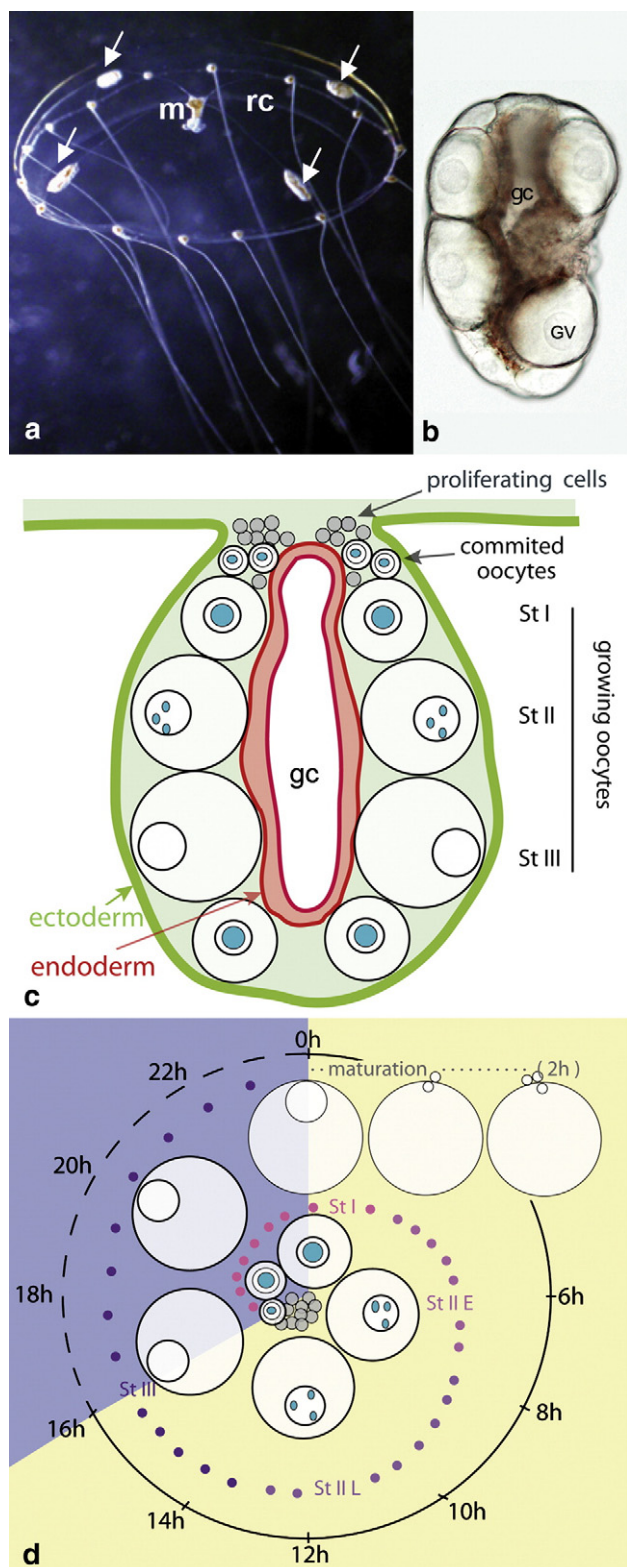


**Fig. 1.** Oogenesis in *Clytia*. (a) An adult *Clytia hemisphaerica* medusa, about 1 cm in diameter, showing the position of the four gonads (white arrows) on the radial canals (rc), which distribute digestion products from the manubrium/stomach (m). (b) Isolated gonad. gc = gastroendodermal cavity; GV = germinal vesicle (c) Diagram of oocyte organization within the female gonad. The growing oocytes lie sandwiched between a flattened endodermal pouch hanging from the radial canal (red) and an ectodermal cell layer (green). In young medusae, dividing cells and small oocytes are positioned proximally with respect to the medusae umbrella. Stage I, II and III growing oocytes are found more distally, although their progression is not strictly ordered. gc: gastroendodermal cavity. (d) Summary of oocyte growth kinetics, based on the data in Table 1: Time is indicated in hours after the light signal for spawning (h.p.l.). Pink and purple dots indicate the oocyte growth period (stages I, II early, II late and III). At 15–16 h.p.l. the oocytes are competent to mature in response to light (yellow background) following a dark period of 2 h or more (blue background: the 8 h dark period of our standard culture conditions is schematised). Oocyte maturation is completed in 2 h.

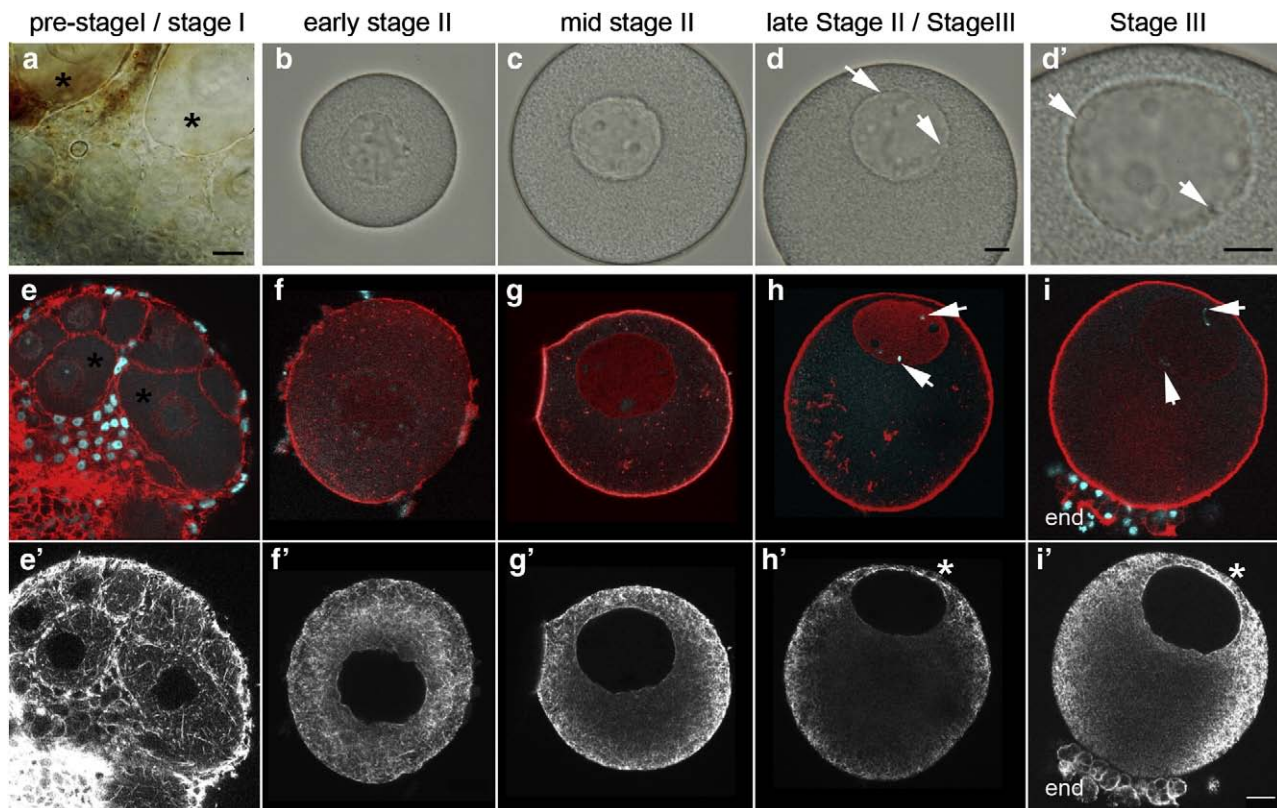


**Fig. 2.** Stages of oocyte growth. (a–d, d') DIC images of living oocytes within an isolated gonad (a) or after isolation (b–d, d'); (e–i) Overlaid confocal images of fixed samples stained with Hoechst dye to visualize DNA (blue) and rhodamine-phalloidin to label polymerized actin (red), with corresponding anti-tubulin immunofluorescence to visualize the microtubule network (e'–i'). The gonad regions shown in a and e/e' are positioned with pre-meiotic and early meiotic stages occupying proximal gonad positions at the bottom, and early stage I growing oocytes positioned more distally towards the top (asterisks). The single large nucleolus of stage I oocytes, characterized by a lack of actin, becomes progressively fragmented during stages II and III. The diplotene chromosomes of growing oocytes are partly decondensed during stage I, but condense to become sharply individualized at the end of the growth period (white arrows in d/d', h, i). The GV is central during the initial period of growth, becomes eccentric during stage II (c, g/g', h/h'), and is positioned close to the oocyte animal surface (top) at stage III (d/d', i/i'), opposite residual attached endoderm cells (end). No major a–v polarity was detected in the distribution of polymerized actin in the cortex or of the microtubule network (e'–i') at any stage of oocyte growth, although the microtubule network appeared to become relatively sparse in central regions as vitellogenesis proceeded, and slightly enhanced between the animally positioned GV and the cortex (asterisks in h' and i'). Scale bars all 20  $\mu$ m.

dispersed and compact, individualized diplotene chromosomes detected (Fig. 2d/d', i).

As shown in Table 1, stage I oocytes were found at all times during the light–dark cycle. In contrast, stage II and stage III oocytes were essentially absent from gonads immediately after light-induced spawning. Stage II oocytes were first detected 4 h after the light signal (h.p.l. = hours post light), 2 h after spawning of the previous generation of oocytes (see Fig. 1d). Starting around 13 h.p.l., gonads became enriched in stage III oocytes at the expense of stage II oocytes. By stimulating meiotic maturation by treating isolated gonads with Br-cAMP (Freeman and Ridgway, 1988), we determined that growing oocytes become competent to mature around 15–16 h after the previous light-stimulation for ovulation, i.e. 2–3 h after stage III oocytes could first be detected (data not shown). Analysis of a large population of oocytes isolated during the growth period revealed a tight correlation between oocyte size and polarity (Table 2): All

oocytes with diameters greater than 140  $\mu$ m showed some polarity and all oocytes over 160  $\mu$ m in diameter had peripheral GV's.

These various observations, summarized in Fig. 1d, indicate that in *Clytia* a sub-population of stage I oocytes becomes committed to growth after each daily spawning. Oocyte growth occurs fairly synchronously between 4 and 18 h.p.l., the first fully-grown and maturation-competent oocytes appearing at 15–16 h.p.l. Relocation of the GV to the animal pole thus occurs during the final period of oocyte growth, a–v polarity being oriented in relation to the underlying endoderm and overlying ectoderm.

*Polarization during oocyte growth requires microtubules*

To address the cellular basis of oocyte polarity development, we examined the organization of microtubules and polymerized actin in isolated gonads and oocytes fixed at different times of the growth

**Table 1**  
Daily progression of oocyte growth in *Clytia* following light-stimulated ovulation

	% Oocytes <sup>a</sup> at each time (hours post light-stimulus)						
	2h	4h	7h	13h	16h	18h	20h
Stage I	97%	47%	58%	52%	53%	52%	67%
Stage II early	3%	31%	29%	0	11%	3%	2%
Stage II late	0	22%	13%	21%	11%	18%	10%
Stage III	0	0	0	27%	25%	27%	21%
Number of oocytes	31	32	31	29	28	33	48

<sup>a</sup> Oocytes isolated from groups of 4 gonads.

**Table 2**  
Correlation between GV position and oocyte size

Nuclear position	Number of oocyte with given diameter ( $\mu$ m) <sup>a</sup>							total
	<120	120–130	130–140	140–150	150–160	160–170	170–180	
GV central	142	11	7	0	0	0	0	160
GV off center	0	12	3	16	6	0	0	37
GV at periphery	0	0	0	7	5	23	0	35
Total	142	23	10	23	11	23	23	232

<sup>a</sup> Oocytes isolated from 28 gonads between 2 h and 20 h after the light signal stimulus.

period. No obvious polarity in the microtubule network or nucleation center was detected at any stage (Figs. 2e'–i'). In previtellogenic oocytes and stage I and stage II growing oocytes, microtubules were detected throughout the cytoplasm, extending from a thin perinuclear layer around the GV throughout the cytoplasm to the cell cortex (Figs. 2e'–g'). During later stages of vitellogenesis (mid-late stage II and stage III), microtubule staining was enhanced in peripheral regions, likely reflecting the higher density of yolk in the center of the oocyte (Figs. 2g'–i'). The microtubule network in fully grown oocytes appeared homogenous around the cell periphery, with a slight enhancement between the GV and the animal cortex (Figs. 2h', i'). The distribution of mitochondria also appeared homogenous throughout the oocyte cytoplasm during oocyte growth, as revealed by vital staining techniques (data not shown). Rhodamine phalloidin staining of polymerized actin produced uniform cortical staining at all stages of oocyte growth (Figs. 2e–i). In stage I oocytes, intense staining was also observed within the GV but excluded from the nucleolus (Fig. 2e). At stage II, a filamentous network could be detected within the GV (Fig. 2f), which was replaced by more uniform phalloidin staining at later stages of oocyte growth (Figs. 2g–i).

To test the involvement of microtubules in oocyte polarization, we cultured isolated gonads in nocodazole during the oocyte growth period and monitored the position of the GV. The complete depolymerization of oocyte cytoplasmic microtubules by nocodazole was confirmed by immunofluorescence staining with anti-tubulin

antibodies (data not shown; see Fig. 7p/q). Treatment of isolated gonads with nocodazole prior to 6 h.p.i. was found to compromise oocyte growth (data not shown), however oocytes in gonads treated from 6 to 13 h.p.i. reached the same size as in controls (Figs. 3a, b), indicating that the latter stages of vitellogenesis are microtubule independent. In these oocytes, the GV failed to relocate to the animal cortex (Figs. 3a, b), indicating that an intact microtubule network is required for this first visible manifestation of a–v polarity in *Clytia* oocytes. Given that oocyte growth is completed in the absence of microtubules, relocation of the GV is unlikely to be driven by asymmetric yolk uptake, although this polarization event may involve microtubule-dependent redistribution of yolk, as has been described in *Xenopus* (Danilchik and Gerhart, 1987).

The role of microfilaments during oocyte growth could not be addressed because treatments of isolated gonads with the microfilament-disrupting drugs Cytochalasin B or Lantrunculin B caused rapid dissociation of the gonad tissues.

#### *A first phase of maternal mRNA polarization during oocyte growth*

Three functionally-characterized, maternally-localized Wnt pathway mRNAs show distinct localizations in the unfertilized *Clytia* egg: CheFz1 RNA shows a cytoplasmic gradient, decreasing from the animal to vegetal pole, while CheWnt3 mRNA is tightly localized to the animal cortex and CheFz3 mRNA to the vegetal cortex (Momose and Houliston, 2007; Momose et al., 2008; Figs. 4f, l, r). To determine exactly when these mRNAs adopt their polarized distributions, we monitored their localization at different stages of oocyte growth by *in situ* hybridization (Fig. 4A left half). Up to stage II, all three mRNAs were detected throughout the cytoplasm, most concentrated around the GV (Figs. 4a, b, g, h, m, n). The *in situ* hybridization signal decreased progressively during vitellogenesis for each mRNA, reflecting yolk accumulation in the cytoplasm. The first RNA to show a polarized distribution was CheFz1 mRNA, which at stage III was found to have become enriched in the animal half of the oocyte relative to the vegetal half, between the GV and the cortex (Fig. 4c; see also Fig. 3c). The distributions of CheFz3 and CheWnt3 mRNAs at this stage showed no a–v polarity, but an irregular patchy distribution in peripheral regions of the oocyte (Figs. 4i, o). Thus the cytoplasmic RNA CheFz1, but not the cortical RNAs CheFz3 and CheWnt3, becomes localized in parallel with GV repositioning during the late-vitellogenic period of oogenesis.

To test whether CheFz1 mRNA localization, like GV repositioning, involves microtubules, we cultured gonads in nocodazole during the growth period and then performed *in situ* hybridization on oocytes isolated from them (Figs. 3c, d). While the cytoplasmic mRNA CheFz1 was found relatively concentrated in the animal hemisphere in 77% of oocytes ( $n=13$ ) from untreated gonads (Fig. 3c), the a–v gradient was largely abolished following nocodazole treatment, with a clear difference in intensity of the *in situ* signal between the animal and vegetal hemispheres observed in only 18% of oocytes ( $n=17$ ). The *in situ* signal typically remained high throughout the cytoplasm following nocodazole treatment (Fig. 3d), suggesting that RNA degradation may contribute to the localization process (see Discussion). Polarization of the oocyte during growth thus involves two microtubule-dependent events, repositioning of the GV and establishment of an a–v gradient of CheFz1 RNA. These events occur in parallel and may reflect direct or independent association of this RNA with the GV, but we cannot exclude the possibility that they occur by independent mechanisms.

#### *Cortical RNA localization is established during oocyte maturation*

The experiments described above define a first phase of polarization of the *Clytia* oocyte, operating during vitellogenesis, which involves microtubule-dependent repositioning of the GV and

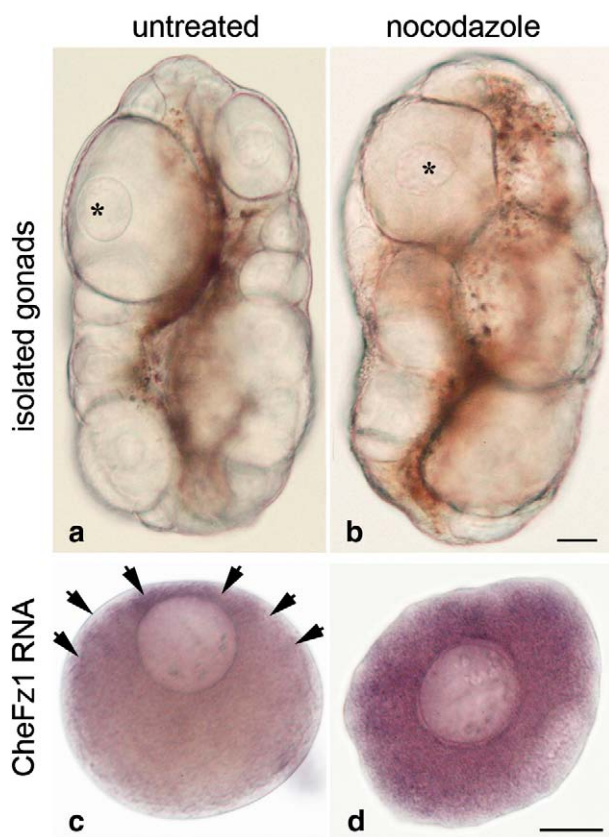


**Fig. 3.** Microtubule dependence of oocyte polarization during growth. Isolated gonads were incubated in 10  $\mu$ M nocodazole to depolymerize microtubules during the later period of growth (from 5 to 13 h after the preceding light stimulus). This nocodazole treatment prevented the polarized repositioning of the GV during oocyte growth, as seen in DIC images of untreated (a) and treated (b) gonads. *In situ* hybridization shows that while CheFz1 mRNA in fully grown oocytes isolated from untreated gonads (c) adopted a graded distribution, being most concentrated between the GV and the cortex in the animal hemisphere (arrows; see also Fig. 4c), oocytes from nocodazole-treated gonads showed high levels of this RNA throughout the oocyte (d). Note that oocyte growth was unaffected by this treatment. Scale bars 50  $\mu$ m.

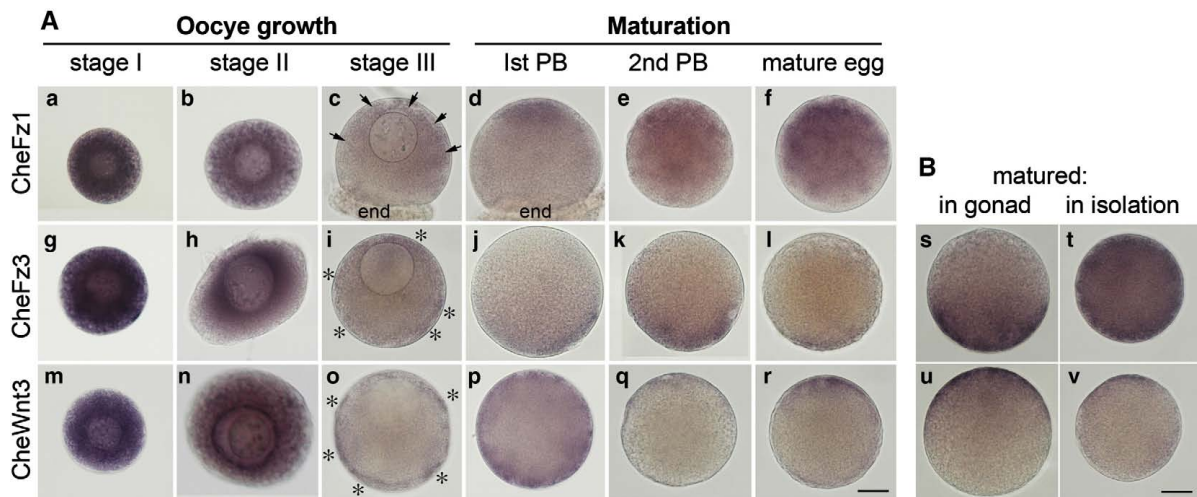


**Fig. 4.** Localization of CheFz1, CheFz3 and CheWnt3 mRNAs during oocyte growth and maturation. (A) *In situ* hybridization detection of CheFz1 mRNA (a–f), CheFz3 mRNA (g–l) and CheWnt3 mRNA (m–r) at successive stages of oocyte growth and maturation, as indicated above the panels. Black arrows in c show that CheFz1 mRNA has already acquired its final animal localization in stage III oocytes. At this stage, CheFz3 and CheWnt3 mRNAs are detected in patches in the peripheral region of the oocyte (asterisks). They only adopt their final polarized distributions during maturation, by first and second polar body (PB) emission respectively. (B) *In situ* hybridization detection of CheFz3 (s, t) and CheWnt3 (u, v) RNAs, following maturation induced by Br-cAMP treatment of intact gonads (s, u) or of isolated oocytes (t, v). Localization of CheWnt3 to the animal cortex has occurred in both contexts, whereas CheFz3 RNA remained uniformly distributed in oocytes matured in isolation but became vegetally concentrated in oocytes matured within gonads. The animal pole is at the top in all stage III and maturing oocytes, opposite any residual attached endoderm cells (end). Scale bars 50  $\mu$ m.

establishment of a cytoplasmic a–v gradient of CheFz1 RNA. This process does not, however, fully account for the polarity of the unfertilized egg, since no a–v polarity was detected in the distribution of CheWnt3 or CheFz3 RNAs at the end of the oocyte growth period. To address the mechanism by which these two RNAs become localized to the animal and vegetal cortex respectively of the unfertilized egg, we monitored their distribution during meiotic maturation (Fig. 4A right half). Maturation was triggered either by culturing isolated gonads through a dark–light cycle or by isolating stage III oocytes manually from the gonads 16 h or more after the previous light stimulus and treating them with Br-cAMP (Freeman and Ridgway, 1988). As reported previously, both methods provoked reproducible and synchronous maturation, with GV breakdown (GVBD) occurring after 10–20 min, first polar body formation after 50–65 min and second polar body formation after 70–95 min (Fig. 5; see Fig. 1d), the spawned egg (110–120 min) being arrested in G1 of the first post-meiotic cell cycle. CheFz3 RNA was found localized in the vegetal cortical region by the time of first polar body emission (Fig. 4j) and CheWnt3 RNA localized to the animal cortex by the time of second polar body emission (Fig. 4q).

In the course of these experiments we noticed that there was a difference in the RNA localization process in oocytes matured in isolation and those matured in intact gonads. While CheWnt3 RNA adopted an equivalent animal localization in oocytes matured alone or within the gonad (84% of 61 cases versus 86% of 58 cases; Figs. 4u, v), CheFz3 RNA failed to adopt its final localization in oocytes matured in isolation (scored as localized in only 6% of 53 cases, compared to 84% of 61 for gonad-matured oocytes). In most isolated oocytes, a strong CheFz3 RNA signal was detected uniformly through the oocyte

cytoplasm following maturation (Fig. 4t). This suggests that the normal localization mechanism for CheFz3 RNA may involve degradation of non-localized RNA in the cytoplasm and animal cortex regions.

Taken together, our observations of CheFz3 and CheWnt3 RNA distribution during oocyte maturation indicate that separable events are responsible for the localization of these RNAs to opposite cortical sites with distinct timing: A first mechanism requiring the presence of gonad tissues, for instance to provide necessary cell contacts and/or soluble factors to stimulate RNA degradation, is responsible for localizing CheFz3 RNA beneath the vegetal cortex. A second, oocyte-autonomous, mechanism targets CheWnt3 RNA to the animal cortex.

*Distinct cytoskeletal requirements for RNA localization during maturation*

To identify cellular reorganizations that could underlie the differential relocation of CheFz3 and CheWnt3 RNAs during oocyte maturation, we examined the organization of microtubules, actin filaments and chromatin in maturing oocytes fixed at successive times following Br-cAMP treatment (Fig. 5). We also made time-lapse recordings of maturing oocytes with DIC optics (Supplementary Movie). The homogenous microtubule network characteristic of the fully-grown oocyte (Fig. 2i' and Fig. 5f) was replaced during the early stages of maturation by an aster nucleated on the vegetal side of the GV and a less well-organized microtubule accumulation on the animal side (Fig. 5g). During this period, the compact, individualized chromosomes of the mature oocyte gather on the microtubules of the vegetal aster before migrating with the forming spindle to the cell cortex (data not shown). Anastral first meiotic spindles were first

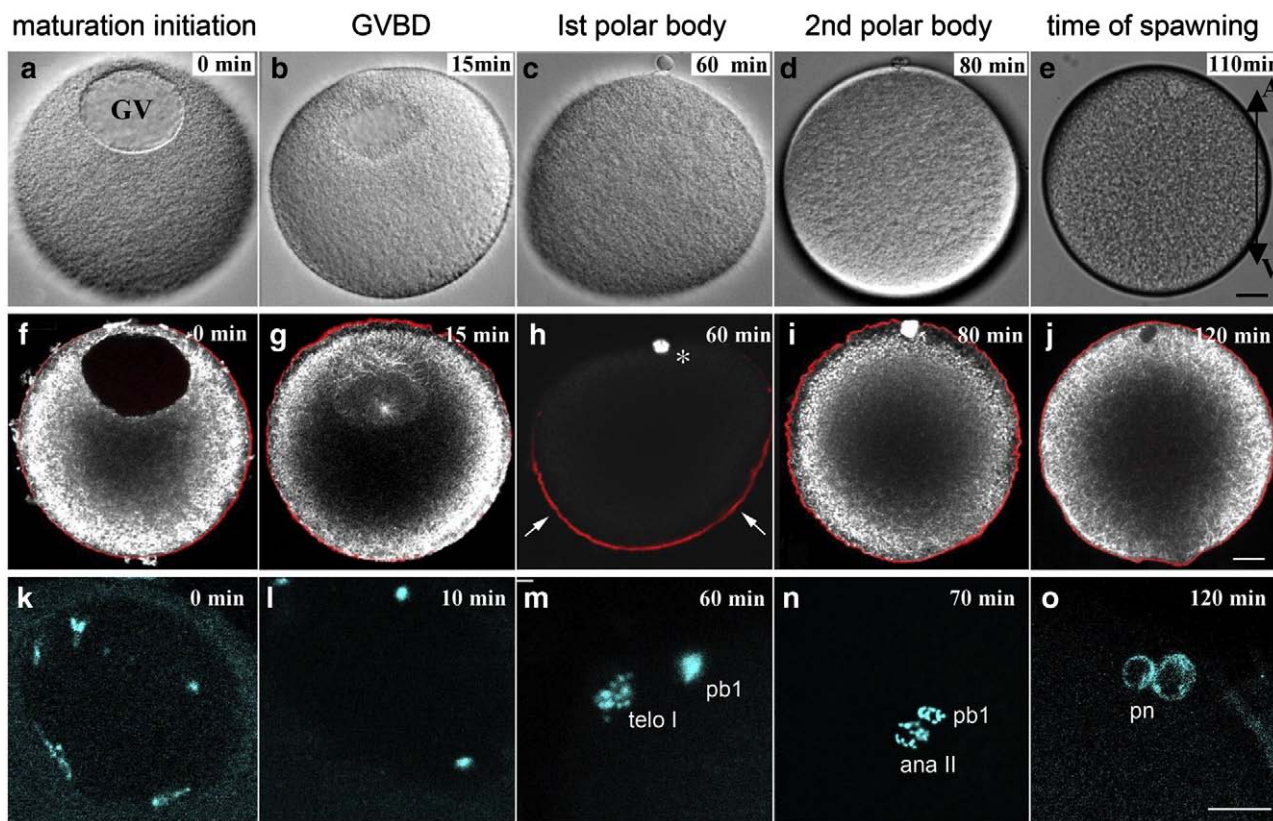


**Fig. 5.** Microtubule and cortical reorganizations during oocyte maturation. Isolated oocytes triggered to mature using Br-cAMP were imaged using DIC optics (a–e) or fixed at successive stages of meiotic maturation as indicated, and labelled for confocal microscopy using anti-tubulin immunofluorescence (white in f–j) and rhodamine-phalloidin (overlaid in red f–j), or Hoechst 33258 to label DNA (k–o). telo I: first meiotic telophase; pb1: first polar body; ana II: second meiotic anaphase; pn: typical bi-lobed female pronucleus. As GVBD occurs (g), the cytoplasmic microtubule network of the stage III oocyte became sparser and one or two cytoplasmic microtubule aster were detected on the vegetal side of the GV, collecting the chromosomes and migrating to the animal cortex, along with a disorganized microtubule structure on the animal side of the GV. Cortical actin becomes transiently polarized during a peristaltic contraction which accompanies first meiosis (arrows in h; Asterisk marks the first meiotic spindle). Scale bars 20  $\mu$ m.

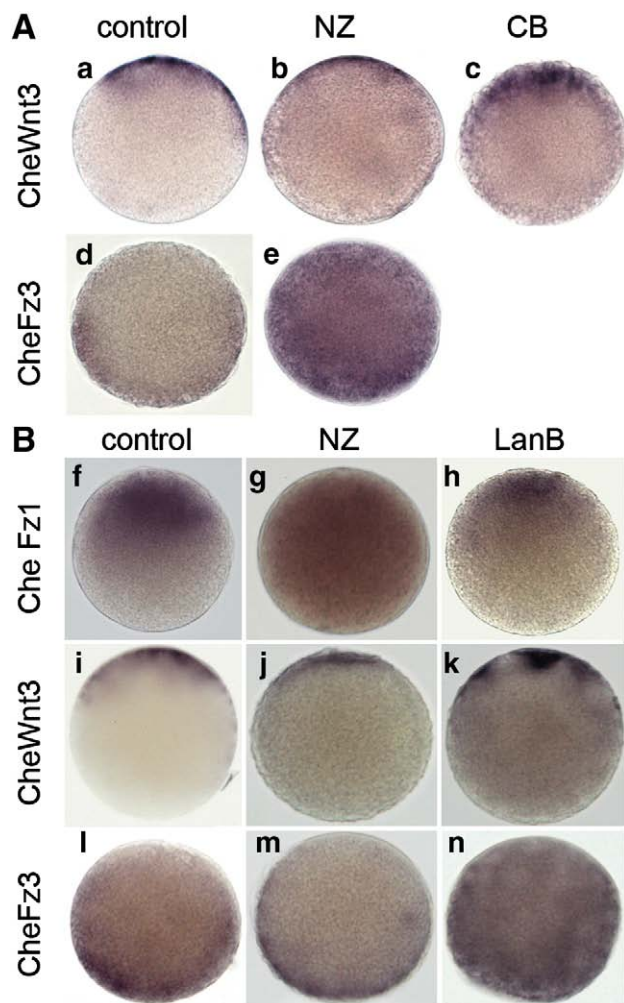


**Fig. 6.** Cytoskeletal requirements for RNA localization and anchorage. (A) Oocytes treated with 10  $\mu$ M nocodazole (NZ) or 10  $\mu$ g/ml cytochalasin B (CB) during Br-cAMP induced maturation and fixed for in situ hybridization for CheWnt3 (a–c) or CheFz3 (d–e). The oocytes shown for CheWnt3 were matured following isolation. Identical results were obtained using intact gonads. For CheFz3 intact gonads were used since localization of this RNA does not occur during maturation in isolated oocytes. The localization of CheFz3 RNA was sensitive to nocodazole during maturation, with high levels of RNA remaining detectable throughout the oocyte rather than only vegetally. CheWnt3 RNA localization to the animal cortex was nocodazole insensitive. CheWnt3 RNA localized to the animal region in the presence of cytochalasin but its distribution was disturbed, probably reflecting cortical disruption. Phenotype percentages are given in Table 3A. (B) Spawned unfertilized eggs treated with 10  $\mu$ M nocodazole (NZ) or 10  $\mu$ g/ml lantrunculin B (LanB) for 30 min and then fixed for in situ hybridization with CheFz1 (f–h), CheWnt3 (i–k) or CheFz3 (l–n) probes. Nocodazole caused dispersal of CheFz1 RNA and appeared to cause loss of residual CheFz3 RNA from cytoplasmic regions, but did not affect the distribution of cortical CheFz3 or CheWnt3 RNA. Lantrunculin B caused partial dispersal of CheFz3 RNA from the vegetal cortex and clumping of CheWnt3 RNA in the animal cortex, but did not affect the cytoplasmic gradient of CheFz1 RNA. Phenotype percentages are given in Table 3B.

detected at the animal pole around 35 min after the onset of maturation, and persisted for a prolonged meiosis I (MI) period (Fig. 5h), as reported in other species (Galas et al., 1993; Polanski et al., 1998). Thus during the meiotic division period when the two cortical RNAs become localized, the general cytoplasmic microtubule network disassembled and microtubules were detectable only in anally located meiotic apparatus (Fig. 5h). A dense, homogenous, microtubule network reformed after completion of the second polar body (Figs. 5i, j).

Time lapse recordings of Br-cAMP stimulated oocytes revealed an exaggerated animal–vegetal cortical contraction wave during the 30–40 min MI period between GVBD and first polar body emission

(Supplementary Movie). A similar but less pronounced contraction was detectable prior to second polar body emission. Rhodamine phalloidin staining (red in Figs. 5f–j) revealed a homogenous cortical actin distribution at all stages of maturation, except during the pronounced MI contraction wave. At this time, strongly polarized actin distributions could be detected along the a–v axis, phalloidin staining being enhanced in the vegetal cortex at the time of first polar body emission (Fig. 5h).

To summarize, asymmetries in the organization of both actin and microtubules during the meiotic divisions are detectable during the localization period for CheFz3 and CheWnt3 RNAs. The pronounced animal–vegetal contraction wave during MI is accompanied by a dramatic transient redistribution of cortical actin, while microtubules become essentially restricted to the anally located meiotic apparatus of both divisions. Treatments with nocodazole (of intact gonads for detection of CheFz3 RNA and of isolated oocytes for detection of CheWnt3 RNA) and cytochalasin B (of isolated oocytes, possible for CheWnt3 RNA only) were used to test the roles of microtubules and microfilaments in CheFz3 and CheWnt3 mRNA localization (Fig. 6A). Neither drug blocked the meiotic chromatin condensation–decondensation cycles although as expected both prevented polar body emission (not shown). CheFz3 mRNA localization was found to be disrupted by nocodazole treatment, this RNA being scored as localized in only 39% of oocytes compared with 81% in untreated controls (Fig. 6e; Table 3A). In contrast, the animal localization of CheWnt3 RNA during maturation was not prevented by treatment of gonads with either nocodazole (in 93% of cases;  $n=24$ ) or cytochalasin B (in 100% of cases;  $n=14$ ) (Fig. 6bc), although a marked broadening of the zone of CheWnt3 localization was observed following maturation in the presence of cytochalasin B (Fig. 6c). These drug experiments indicate that microtubules contribute to the gonad-dependent process of CheFz3 localization, perhaps contributing to RNA degradation, as hypothesized for CheFz1 during oocyte growth (see above), but not for the oocyte-autonomous CheWnt3 mRNA localization during the meiotic division period. Microfilaments are not required for the localization CheWnt3 RNA to the animal cortex but, not unexpectedly, appear to contribute to its regular distribution in this region.

*Distinct mechanisms maintain RNA localization in the unfertilized egg*

To investigate the mechanisms involved in maintaining the three differentially localized RNAs at their final destinations we treated mature unfertilized eggs with cytoskeletal inhibitors for 30 min and

**Table 3**  
Effect of cytoskeletal inhibitors on RNA localization and anchoring

Localized RNA	A: Treatment during maturation		
	Untreated	Nocodazole	Cytochalasin B
CheWnt3	96%	93%	100% <sup>a</sup>
<i>n</i>	79	24	14
CheFz3	81%	39%	–
<i>n</i>	84	33	–
B: Treatment of mature eggs			
	Control	Nocodazole	Lantrunculin B
CheFz1	67%	47%	72%
<i>n</i>	24	17	18
CheWnt3	100%	100%	100% <sup>b</sup>
<i>n</i>	26	18	30
CheFz3	76%	82%	71% <sup>c</sup>
<i>n</i>	33	27	35

For the criteria used for assessing RNA localization, see Materials and methods.

<sup>a</sup> RNA concentrated in animal hemisphere but more widely distributed than controls (Fig. 6f).

<sup>b</sup> RNA with clumpy distribution in the animal cortex (Fig. 6n).

<sup>c</sup> Additional RNA dispersed in the cytoplasm (Fig. 6q)

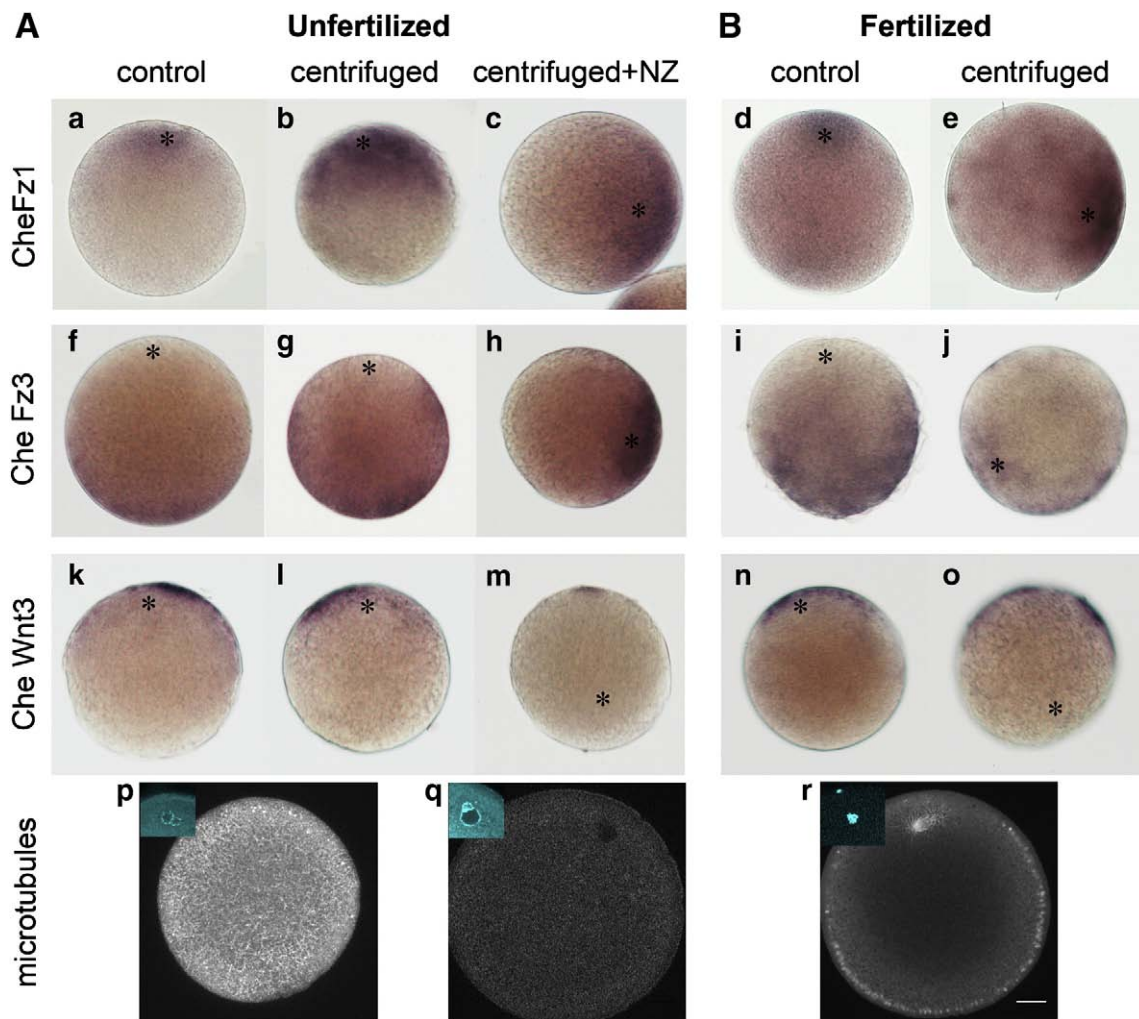


**Fig. 7.** Anchoring of localized RNAs tested by low-speed centrifugation. (A) Unfertilized eggs were centrifuged in the absence or presence of nocodazole (NZ) and then fixed for *in situ* hybridization with CheFz1 (a–c), CheFz3 (f–h) or CheWnt3 (k–m) probes. The position of the nucleus is marked by an asterisk. Note that although there is no independent marker for a–v polarity, the images of untreated centrifuged eggs have been oriented with the nucleus at the top because the relative positions of the nuclei and RNA were not altered under these conditions (see quantification in Table 4). In contrast, centrifugation in the presence of nocodazole disturbed the position of the nuclei with respect to the cortical CheFz3 and CheWnt3 RNAs indicating that the nuclei were displaced, so the images have been oriented with respect to RNA rather than nuclear position. In these conditions CheFz1 RNA and CheFz3 RNAs were found consistently on the same side as the nucleus, indicating that they also were displaced by the centrifugal force, while CheWnt3 RNA appeared to remain cortically anchored. (B) Equivalent centrifugation of fertilized eggs. As in nocodazole-treated unfertilized eggs, CheFz1 RNA (d,e) was found consistently on the same side as the nucleus following centrifugation. In contrast, CheFz3 RNA (i,j), like CheWnt3 RNA (n,o) showed behavior consistent with cortical anchoring. p–r: Immunofluorescence staining with anti-tubulin antibodies shows that the dense microtubule network of unfertilized eggs (p) is completely undetectable following nocodazole treatment (q), while fertilized eggs contain a residual cortical network at the time of first mitosis (r). Inserts show Hoechst staining of DNA. Scale bars 20  $\mu$ m.

**Table 4**  
Effects of centrifugation on RNA localization

	RNA localization following centrifugation					
	CheFz1 with nucleus <sup>a</sup>		CheFz3 opposite nucleus <sup>b</sup>		CheWnt3 with nucleus <sup>a</sup>	
<i>Unfertilized</i>	Untreated	Nocodazole	Untreated	Nocodazole	Untreated	Nocodazole
Control	100%	(delocalized)	100%	100%	100%	96%
n	17	17	14	15	23	27
Centrifuged	73%	74%	82%	0% <sup>c</sup>	92%	8% <sup>d</sup>
n	22	15	18	15 <sup>c</sup>	26	15 <sup>d</sup>
<i>Fertilized</i>	Untreated		Untreated		Untreated	
Control	100%		100%		100%	
n	25		23		31	
Centrifuged	100%		36% <sup>d</sup>		45% <sup>d</sup>	
n	64		25 <sup>d</sup>		40 <sup>d</sup>	

<sup>a</sup> Nucleus positioned within a 90° segment centred on the RNA staining.

<sup>b</sup> Nucleus is positioned within a 90° segment opposite the RNA staining.

<sup>c</sup> In all these eggs the CheFz3 RNA coincided with the nucleus (See Fig. 7j).

<sup>d</sup> In these eggs the position of the RNA staining was variable with respect to the nucleus.

then examined RNA distribution by *in situ* hybridization (Fig. 6B; Table 3). Nocodazole treatment resulted in partial or complete dispersion of CheFz1 RNA through the cytoplasm (Fig. 6g). The cortical localization of CheWnt3 and CheFz3 RNAs (Fig. 6j,m) was not affected by nocodazole treatment, although a decrease in the residual cytoplasmic signal was consistently observed for CheFz3 RNA. In contrast, treatment of unfertilized eggs with the microfilament-disrupting drug lantrunculin B caused CheFz3 RNA to spread widely through the egg cytoplasm (Fig. 6n), while CheWnt3 RNA distribution in the animal cortex was disrupted into irregular patches (Fig. 6k). This drug had no detectable effect on the CheFz1 RNA gradient in the cytoplasm (Fig. 6h).

mRNA anchoring in mature unfertilized eggs was tested further by low-speed centrifugation (Fig. 7A; Table 4), using conditions that cause nuclear displacement in fertilized *C. gregarium* eggs (Freeman, 1981a,b; see below for confirmation in fertilized *C. hemisphaerica* eggs). In *C. hemisphaerica* the polar bodies are lost following fertilization leaving no external marker for a–v polarity. We therefore assessed the effect of the centrifugation by comparing the position of each RNA with that of the nucleus. In the absence of cytoskeletal inhibitors, the distinct relationships of all three mRNA tested with respect to the nucleus were maintained following centrifugation (Figs. 7b, g, l; Table 4), indicating that both the nucleus and the RNAs are stably anchored. Following depolymerization of the dense microtubule network using nocodazole (Figs. 7p, q), however, centrifugation altered the relationship between the nuclei and the two cortically localized RNAs (Figs. 7h, m; Table 4). In the case of CheWnt3 RNA, the relative position of the nucleus and RNA was randomized (Fig. 7m), consistent with relocation of the nucleus in to the centrifugal field while the RNA remained cortically anchored. In contrast, CheFz3 mRNA consistently re-localized to coincide with the nucleus (Fig. 7h), indicating clearly that it was displaced in the centrifugal field in parallel with the nucleus. The cytoplasmic RNA CheFz1 was similarly found localized on the same side as the nucleus following nocodazole treatment and centrifugation (Fig. 7c). We conclude that these two RNAs are associated with a dense structure sensitive to low-speed centrifugation, which may be the nucleus itself or independent of it. Maintenance of CheFz1 RNA in the animal cytoplasm and of CheFz3 RNA in the vegetal cortex of unfertilized eggs, as well as the position of nucleus, involves an intact microtubule network, while CheWnt3 anchoring in the animal cortex is microtubule independent. Since CheFz3 RNA does not redistribute upon simple nocodazole incubation (Fig. 6m) additional structures sensitive to centrifugation likely participate in retaining it in the vegetal region.

Taken together with our analyses of RNA localization during maturation, these centrifugation experiments indicate that the localization and maintenance in distinct cytoplasmic and cortical regions of the oocyte for CheFz1 RNA and for CheFz3 RNA involves microtubules, while CheWnt3 localization and anchoring to the

vegetal cortex is microtubule independent. Not unexpectedly, the distribution of RNAs in cortical regions of both animal and vegetal hemispheres is affected by disrupting actin organization.

#### Centrifugation of fertilized eggs selectively relocates CheFz1 RNA

Experiments using *C. gregarium* showed that egg a–v polarity and the future oral–aboral axis of the embryo can be uncoupled by low-speed centrifugation of fertilized eggs (Freeman, 1980, 1981a). The resulting conclusion, that polarity cues for embryogenesis are set up at the time of first cleavage with respect to the first cleavage site, is difficult to reconcile with the identification in *C. hemisphaerica* of pre-localized RNAs (CheFz1 and CheFz3) that act as axis determinants (Momose and Houlston, 2007). We thus examined the distribution of these RNAs in fertilized eggs by *in situ* hybridization following centrifugation (Fig. 7B). We were assured that the nucleus was displaced randomly under these experimental conditions by the loss of its relationship with CheFz3 and CheWnt3 RNAs (Figs. 7j, o; Table 4). The variable position of these cortical RNAs with respect to the nucleus following centrifugation indicated that they both remained anchored during nuclear displacement. In contrast, the cytoplasmic RNA CheFz1 consistently became positioned on the same side of the egg as the nucleus following centrifugation (Fig. 7e; Table 4) indicating that it was displaced centrifugally in the same manner as the nucleus. This mirrors the situation in unfertilized eggs in which microtubules have been depolymerized using nocodazole (Fig. 7c), likely reflecting the physiological microtubule depolymerization during the first cell cycle (Fig. 7r). The maintenance of CheFz3 RNA localization after fertilization could be explained by the presence of residual cortical microtubules.

These data show that CheFz1 RNA, but not the cortical RNAs CheWnt3 and CheFz3, is displaced by centrifugation of fertilized eggs. Since CheFz1 mRNA fulfills the experimental criteria for a polarity determinant in *Clytia* (Momose and Houlston, 2007), its sensitivity to centrifugation could explain, at least in part, a–v axis re-specification by low speed centrifugation.

#### Discussion

In this study we have defined the characteristics of oocyte growth and maturation in a new cnidarian experimental model *Clytia hemisphaerica*, and provide the first analysis of the cellular basis of oocyte polarization in a cnidarian. In *Clytia*, as is typical in bilaterian species; oocyte polarity provides the basic framework for the body plan. The deceptive simplicity of the unfertilized egg hides a remarkable complexity of subcellular polarity, with specific RNAs segregated to three distinct regions contributing to embryonic axis formation (Momose et al., 2008; Momose and Houlston, 2007). We

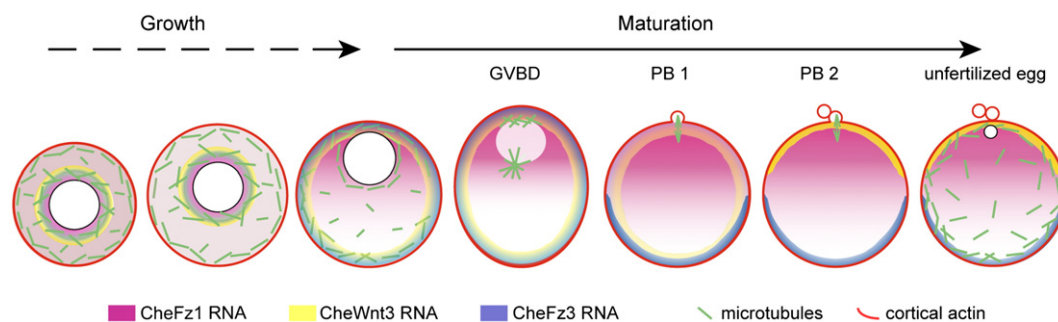


**Fig. 8.** Polarity establishment during oocyte growth and maturation in *Clytia*. Summary of the distinct localization characteristics of each RNA in relation to cytoskeletal organization. The first step in the development of oocyte polarity is the microtubule-dependent relocalization of the GV to the animal pole during oocyte growth. During this period CheFz1 RNA adopts a graded distribution, by a mechanism which may involve preferential stabilization around the GV in the animal hemisphere. During meiotic maturation, CheFz3 RNA becomes concentrated beneath the vegetal cortex and then CheWnt3 RNA adopts its distinct localization at the animal cortex. CheFz3 RNA localization and anchoring requires microtubules, while the animal localization of CheWnt3 RNA is microtubule independent.

have shown that a–v polarity is acquired in successive and mechanistically separable steps, summarized in Fig. 8. The first step occurs during the last few hours of oocyte growth and involves the microtubule-dependent repositioning of the GV to the animal pole and concomitant establishment of a cytoplasmic CheFz1 RNA gradient. Then, when spawning and meiotic completion are triggered, separable processes relocalize the peripherally located CheFz3 and CheWnt3 RNAs to vegetal and animal regions of the cortex respectively. Our analyses show that as in *Drosophila* and *Xenopus*, maternal RNA localization in *Clytia* is achieved by a combination of mechanisms, including microtubule mediated intracellular polarization, anchoring to the actin-rich cortex, extracellular cues, and possibly selective RNA degradation (see below for more detailed discussion). The axis determinant RNA CheFz1 is not tightly anchored in the fertilized egg, and its displacement to the same site as the nucleus upon low-speed centrifugation provides a possible explanation for experimental embryonic axis re-specification.

#### *Polarity development during oocyte growth in Clytia hemisphaerica*

*Clytia* is an experimental model well adapted for analysis of oocyte development, and the discovery of three maternal mRNAs with distinct localizations and functions in axis determination opens the way to comparisons of RNA localization mechanisms between cnidarian and bilaterian models. The complete transparency of gonads and oocytes facilitates imaging of both living and fixed material, while gonads detached from the medusae have a remarkable capacity to undergo successive cycles of oocyte growth and spawning when cultured under an appropriate dark–light regime. Living oocytes at all stages of oogenesis and meiotic maturation are thus accessible to observation and potentially to manipulation, with growing oocytes injectable through the epithelial wall of the gonad (Amiel et al., in press). A similar analysis system involving “umbrella-free medusae” and isolated oocytes has been used to dissect the cAMP response during meiotic maturation in the hydrozoan *Cyrtia uchidae* (Takeda et al., 2006).

In this study we defined the characteristics of oocyte growth in *Clytia* and its relationship with polarity establishment. We found that after each daily spawning, a population of small “stage I” oocytes embarks upon its terminal growth phase. Under our medusa feeding conditions, 2–8 oocytes commit to growth each day, completing growth to stage III after approximately 13–18 h. Stage III oocytes become competent to undergo meiotic maturation about 2 h after their first appearance, similar timing for maturation competence to that defined in *Cyrtia* (Takeda et al., 2006). The first signs of a–v polarity in *Clytia* oocytes are detectable during stages II and III of oocyte growth. The GV becomes progressively repositioned from a central position towards the cell surface, defining the future animal pole. In parallel CheFz1 the mRNA adopts a graded distribution in the cytoplasm, with the highest concentration between the GV and the animal cortex. CheFz1 RNA may associate indirectly with the nucleus, for instance by stabilization on, or association with, the perinuclear microtubules, or more directly via components of the nuclear membrane, as shown for “P granule” RNAs in developing *C. elegans* oocytes (Pitt et al., 2000).

The development of oocyte polarity during oocyte growth in *Clytia* was found to require an intact microtubule network, and to be oriented with respect to the surrounding tissues of the gonad (see Fig. 1c). It thus shows strong parallels with a key event during in *Drosophila* oogenesis, in which dynein and kinesin-mediated reorganizations of the microtubule network are instrumental in displacing and anchoring the GV and associated dorsal determinant RNAs to the future dorsoanterior margin of the oocyte (Duncan and Warrior, 2002; Januschke et al., 2002). Another related event is the polarization of mouse blastomeres at compaction, in which microtubule redistribution is directed with respect to cell contacts and/or enhancement

between cortical and perinuclear networks (Houlston et al., 1989). We could detect no obvious polarity of the microtubule network in growing *Clytia* oocytes, although as in *Drosophila* oocytes and mouse blastomeres an enrichment of microtubules was found around the GV before and after its relocation. A distinct microtubule structure could, however, be distinguished between the animal cortex and the GV shortly after the onset of maturation, in addition to the vegetal-side MTOC. A distinct sub-population of microtubules at the animal pole could participate in attracting or anchoring the GV prior to maturation, as reported in sea cucumber oocytes (Miyazaki et al., 2005).

In *Drosophila* oocytes, adjacent somatic follicle cells provide cues for the establishment of a polarized microtubule network, which mediates the final localization of both anterior and posterior-specific RNAs (Steinhauer and Kalderon, 2006; van Eeden and St Johnston, 1999). In *Clytia*, gastrodermal cells contacting the oocyte on the vegetal side, and/or overlying ectoderm cells, could potentially provide similar external cues for GV re-positioning and RNA localization. Future studies should address the possibility that a subtle polarity in the microtubule network is established at this time, as in *Drosophila* oocytes (Zimyanin et al., 2007). Cell contacts may contribute to oocyte polarity development in *Clytia* through the ovulation period as well as during growth, since CheFz3 mRNA fails to localize during maturation if oocytes are isolated from the gonad (see below).

#### *Polarized mRNA localization is completed during oocyte maturation*

While CheFz1 adopts a polarized distribution as the GV is repositioned animally during the final oocyte growth phase, the two cortical RNAs become evenly distributed through the less yolky peripheral zone of the oocyte. The polarized localizations of these cortical RNAs are achieved by two clearly distinct mechanisms operating during the meiotic divisions, successively targeting CheFz3 mRNA to the vegetal cortex and then CheWnt3 mRNA to the animal cortex (see Fig. 8). Another aspect of oocyte polarization during maturation has been reported in *Hydractinia*, which involves the development of a specialized fertilization site at the animal pole (Freeman, 1987).

The microtubule-dependent process of CheFz3 RNA localization, which is completed by the time of first polar body emission, remains far from fully understood. Our in situ observations suggest that localized RNA degradation may be involved, as described in a number of other RNA localization processes (Bashirullah et al., 1999). This hypothesis requires testing using quantitative methods to measure RNA levels. Microtubule-directed transport appears unlikely to contribute to CheFz3 RNA localization, since microtubules are largely restricted to the animally-positioned meiotic apparatus at this time. Intriguingly, microtubule disruption by nocodazole during maturation appeared to stabilize CheFz3 RNA through the cytoplasm, while nocodazole treatment after maturation promoted its disappearance in the cytoplasm and rendered cortical anchoring sensitive to centrifugation. One possible explanation for these observations is that the microtubules of the meiotic apparatus stimulate CheFz3 RNA degradation directly or indirectly during maturation, whereas the interphase microtubule network that reforms after second polar body emission has a stabilizing influence. Since the CheFz3 RNA localization process fails to occur in isolated oocytes, another hypothesis is that this RNA is selectively stabilized in the vegetal region in relation to an as-yet unidentified contact-driven polarity.

The RNA localization mechanism that targets CheWnt3 RNA to the animal cortex during maturation is oocyte autonomous and microtubule-independent, but was partially impaired by cytochalasin B treatment. The final cortical distribution of CheWnt3 RNA was disturbed by actin-disrupting drugs, although retained its general localization, and also differed from CheFz3 RNA by its insensitivity to nocodazole treatment. The redistribution of CheFz3 and of CheWnt3 RNAs during meiosis show similar timing to the localization of certain

specific RNAs during oocyte maturation in ascidians, driven by an actin-dependent cytoplasmic flow following GVBD (Prodon et al., 2006, 2008). In *Clytia* we observed exaggerated cortical contractions that crossed the oocyte during the period between GVBD and polar body emission, and as in ascidian oocytes these provoked clear counter-movements of the internal cytoplasm. Similar cortical and cytoplasmic rearrangements along the a–v axis have been described to accompany meiosis or mitosis in other organisms, contributing to determinant localization during annelid ooplasmic segregation (Shimizu, 1999) and *Xenopus* egg “Surface Contraction Waves” (Savage and Danilchik, 1993). Actin disrupting drugs in *Clytia* disrupted cortical contractions during meiosis but did not prevent CheWnt3 RNA localization, in contrast to the corresponding ascidian event. This suggests that any dependence on the cortical contraction is only partial. In *Drosophila* oocytes, cytoplasmic flows facilitate entrapment of Nanos RNA to a specialized cortical domain, but are not essential for this process (Forrest and Gavis, 2003; Glotzer et al., 1997). It is possible that cytoplasmic flow during the *Clytia* oocyte MI wave facilitates anchoring of CheWnt3 RNA to an independently established animal cortical domain, or that the transient polarized reinforcements of cortical actin during this wave contribute to the creation of such a domain to which the RNA later anchors or is preferentially stabilized.

#### Maternal determinant anchoring and axis specification

Classic experimental embryology experiments have demonstrated that the embryonic axis in hydrozoans can be re-orientated by displacing the zygote nucleus in fertilized eggs, and that duplication of the nucleus can lead to duplication of the oral pole of the embryo (Freeman, 1980, 1981a,b). These demonstrations that axis orientation is labile after fertilization may at first sight seem incompatible with the presence of maternal axis determinant molecules pre-localized in the unfertilized egg. The two notions can be reconciled, however, by proposing that a dominant axis-determining factor is not cortically anchored as in bilaterian models, but free to become redistributed to the same site as the nucleus during experimental manipulations. Centrifugation could theoretically either reposition animal/oral determinant with the nucleus, or a vegetal/aboral determinant to the opposite side of the oocyte, although the first possibility is clearly favored by the observation that nuclear separation can cause oral pole duplication (Freeman, 1981a).

CheFz1 RNA in *Clytia* eggs is atypical amongst localized RNAs in not showing cortical anchoring, and is a good candidate for a mobile oral determinant. Previous studies have shown that CheFz1 RNA fulfills all the experimental criteria of an oral determinant, being both necessary for oral fate development and sufficient to re-direct axis orientation upon ectopic expression (Momose and Houlston, 2007). We have demonstrated that CheFz1 RNA, unlike CheWnt3 and CheFz3 RNAs, relocates to the same site as the zygote nucleus upon centrifugation. If CheFz1 RNA relocation is indeed responsible for axis specification in manipulated eggs, its effect must be dominant over CheFz3 RNA, which has aboral determinant properties but remains cortically anchored. CheWnt3 RNA also remains cortically anchored, but has been shown not to have a directive role in the first phase of axis specification (Momose et al., 2008). CheFz1 RNA may not be the only factor contributing to axis re-specification upon nuclear displacement or duplication. Maternal RNAs and/or proteins for other Wnt pathway regulators such as Dishevelled,  $\beta$ -catenin or TCF could also be relocalized experimentally. Dishevelled protein has been shown to localize to the first cleavage site in *Nematostella* eggs (Lee et al., 2007). Another possibility is that the protein product of the cortically anchored RNA CheWnt3 rapidly associates with the zygote nucleus following its translation after fertilization.

It is clear from our study that the acquisition of oocyte polarity in the cnidarian *Clytia* is a multi-step process sharing common features with that in *Drosophila*, *Xenopus* and ascidian oocytes (King et al.,

2005; Micklem, 1995; Sardet et al., 2007). Although much remains to be understood about RNA localization in *Clytia*, our initial characterization indicates that it involves a number of distinct mechanisms from the repertoire described in other models, including microtubule-mediated nuclear relocation, selective RNA degradation, anchoring at specialized sites and meiosis-related cortical/cytoplasmic flows (Bashirullah et al., 1999; Forrest and Gavis, 2003; Chang et al., 2004; Prodon et al., 2008). Differences in the behavior of determinants upon experimental manipulation in hydrozoan and bilaterian models may be consequences of differences in the deployment of RNA anchoring mechanisms.

#### Acknowledgments

We thank C. Sardet, T. Momose, P. Chang, S. Chevalier, C. Fourrage, E. Roettinger and F. Prodon for experimental help, stimulating discussions and useful comments on the manuscript, and T. Momose for Fig. 1a. Work was financed by the ANR, the CNRS and by MRT and ARC studentships to A.A.

#### Appendix A. Supplementary data

Supplementary data associated with this article can be found, in the online version, at doi:10.1016/j.ydbio.2008.12.007.

#### References

- Amiel, A., Leclère, L., Robert, L., Chevalier, S., Houlston, E., in press. Conserved functions for Mos in eumetazoan oocyte maturation revealed by studies in a cnidarian. *Current Biology*.
- Bashirullah, A., Halsell, S.R., Cooperstock, R.L., Kloc, M., Karaiskakis, A., Fisher, W.W., Fu, W., Hamilton, J.K., Etkin, L.D., Lipshitz, H.D., 1999. Joint action of two RNA degradation pathways controls the timing of maternal transcript elimination at the midblastula transition in *Drosophila melanogaster*. *EMBO J.* 18, 2610–2620.
- Chang, P., Torres, J., Lewis, R.A., Mowry, K.L., Houlston, E., King, M.L., 2004. Localization of RNAs to the mitochondrial cloud in *Xenopus* oocytes through entrapment and association with endoplasmic reticulum. *Mol. Biol. Cell* 15, 4669–4681.
- Chevalier, S., Martin, A., Leclère, L., Amiel, A., Houlston, E., 2006. Polarised expression of FoxB and FoxQ2 genes during development of the hydrozoan *Clytia hemisphaerica*. *Dev. Genes Evol.* 216, 709–720.
- Danilchik, M.V., Gerhart, J.C., 1987. Differentiation of the animal–vegetal axis in *Xenopus laevis* oocytes. I. Polarized intracellular translocation of platelets establishes the yolk gradient. *Dev. Biol.* 122, 101–112.
- Di Carlo, M., 2004. Paracentrotus lividus eggs contain different RNAs at the animal and vegetal poles. *Biochem. Biophys. Res. Commun.* 315, 1110–1119.
- Duncan, J.E., Warrior, R., 2002. The cytoplasmic dynein and kinesin motors have interdependent roles in patterning the *Drosophila* oocyte. *Curr. Biol.* 12, 1982–1991.
- Faulkner, 1929. The early prophase of the first oocyte division as seen in life, in *Obelia geniculata*. *Q. J. Microsc. Sci.* s2–73, 225–242.
- Forrest, K.M., Gavis, E.R., 2003. Live imaging of endogenous RNA reveals a diffusion and entrapment mechanism for nanos mRNA localization in *Drosophila*. *Curr. Biol.* 13, 1159–1168.
- Freeman, G., 1976. The role of cleavage in the localization of developmental potential in the ctenophore *Mnemiopsis leidyi*. *Dev. Biol.* 49, 143–177.
- Freeman, G., 1977. The establishment of the oral–aboral axis in the ctenophores. *J. Embryol. Exp. Morphol.* 42, 237–260.
- Freeman, G., 1980. The role of cleavage in the establishment of the anterior–posterior axis of the hydrozoan embryo. In: Tardent, P., Tardent, R. (Eds.), “Developmental and Cellular Biology of Coelenterates”. Elsevier/North Holland Biomedical press, pp. 97–108.
- Freeman, G., 1981a. The cleavage initiation site establishes the posterior pole of the hydrozoan embryo. *Wilhelm Roux Arch.* 190, 123–125.
- Freeman, G., 1981b. The role of polarity in the development of the hydrozoan planula larva. *Wilhelm Roux Arch.* 190, 168–184.
- Freeman, G., 1987. The role of oocyte maturation in the ontogeny of the fertilization site in the hydrozoan *Hydractinia echinata*. *Roux's Arch. Dev. Biol.* 196, 83–92.
- Freeman, G., Ridgway, E.B., 1988. The role of cAMP in oocyte maturation and the role of the germinal vesicle contents in mediating maturation and subsequent developmental events in hydrozoans. *Roux's Arch. Dev. Biol.* 197, 197–211.
- Fritzenwanker, J.H., Genikhovich, G., Kraus, Y., Technau, U., 2007. Early development and axis specification in the sea anemone *Nematostella vectensis*. *Dev. Biol.* 310, 264–279.
- Galas, S., Barakat, H., Doree, M., Picard, A., 1993. A nuclear factor required for specific translation of cyclin B may control the timing of first meiotic cleavage in starfish oocytes. *Mol. Biol. Cell* 4, 1295–1306.
- Galliot, B., Schmid, V., 2002. Cnidarians as a model system for understanding evolution and regeneration. *Int. J. Dev. Biol.* 46, 39–48.

- Glotzer, J.B., Saffrich, R., Glotzer, M., Ephrussi, A., 1997. Cytoplasmic flows localize injected oskar RNA in *Drosophila* oocytes. *Curr. Biol.* 7, 326–337.
- Hargitt, G.T., 1919. Germ cells of coelenterates. VI General considerations, discussion, conclusions. *J. Morph.* 33, 1–58.
- Henry, J.Q., Perry, K.J., Wever, J., Seaver, E., Martindale, M.Q., 2008. beta-Catenin is required for the establishment of vegetal embryonic fates in the nemertean, *Cerebratulus lacteus*. *Dev. Biol.* 317, 368–379.
- Honegger, T.G., Achermann, J., Littlefield, R.J., Baenninger, R., Tardent, P., 1980. Light-controlled spawning in *Phialidium hemisphaericum* (Leptomedusae). In: Tardent, P., Tardent, R. (Eds.), "Developmental and Cellular Biology Of Coelenterates: Proceedings IV International Coelenterate Conference". Elsevier/N. Holland Biomedical Press, Amsterdam, pp. 83–88.
- Horstadius, S., 1953. The effect of lithium ions in centrifuged eggs of *Paracentrotus lividus*. *Pubbl. Stn. Zool. Napoli* 24, 45–60.
- Houliston, E., Pickering, S.J., Maro, B., 1989. Alternative routes for the establishment of surface polarity during compaction of the mouse embryo. *Dev. Biol.* 134, 342–350.
- Houliston, E., Carré, D., Johnston, J.A., Sardet, C., 1993. Axis establishment and microtubule-mediated waves prior to first cleavage in *Beroë ovata*. *Development* 117, 75–87.
- Imai, K., Takada, N., Satoh, N., Satou, Y., 2000. (beta)-catenin mediates the specification of endoderm cells in ascidian embryos. *Development* 127, 3009–3020.
- Januschke, J., Gervais, L., Dass, S., Kaltschmidt, J.A., Lopez-Schier, H., Johnston, D.S., Brand, A.H., Roth, S., Guichet, A., 2002. Polar transport in the *Drosophila* oocyte requires Dynein and Kinesin I cooperation. *Curr. Biol.* 12, 1971–1981.
- King, M.L., Messitt, T.J., Mowry, K.L., 2005. Putting RNAs in the right place at the right time: RNA localization in the frog oocyte. *Biol. Cell.* 97, 19–33.
- Lee, P.N., Kumburegama, S., Marlow, H.Q., Martindale, M.Q., Wikramanayake, A.H., 2007. Asymmetric developmental potential along the animal–vegetal axis in the anthozoan cnidarian, *Nematostella vectensis*, is mediated by Dishevelled. *Dev. Biol.* 310, 169–186.
- Marlow, H.Q., Martindale, M.Q., 2007. Embryonic development in two species of scleractinian coral embryos: symbiodinium localization and mode of gastrulation. *Evol. Dev.* 9, 355–367.
- Micklem, D.R., 1995. mRNA localisation during development. *Dev. Biol.* 172, 377–395.
- Miyazaki, A., Kato, K.H., Nemoto, S., 2005. Role of microtubules and centrosomes in the eccentric relocation of the germinal vesicle upon meiosis reinitiation in sea-cucumber oocytes. *Dev. Biol.* 280, 237–247.
- Momose, T., Schmid, V., 2006. Animal pole determinants define oral–aboral axis polarity and endodermal cell-fate in hydrozoan jellyfish *Podocoryne carnea*. *Dev. Biol.* 292, 371–380.
- Momose, T., Houliston, E., 2007. Two oppositely localised frizzled RNAs as axis determinants in a cnidarian embryo. *PLoS Biol.* 5, e70.
- Momose, T., Derelle, R., Houliston, E., 2008. A maternally localised Wnt ligand required for axial patterning in the cnidarian *Clytia hemisphaerica*. *Development* 135, 2105–2113.
- Nishida, H., 2005. Specification of embryonic axis and mosaic development in ascidians. *Dev. Dyn.* 233, 1177–1193.
- Pitt, J.N., Schisa, J.A., Priess, J.R., 2000. P granules in the germ cells of *Caenorhabditis elegans* adults are associated with clusters of nuclear pores and contain RNA. *Dev. Biol.* 219, 315–333.
- Plickert, G., Jacoby, V., Frank, U., Muller, W.A., Mokady, O., 2006. Wnt signaling in hydroid development: formation of the primary body axis in embryogenesis and its subsequent patterning. *Dev. Biol.* 298, 368–378.
- Polanski, Z., Ledan, E., Brunet, S., Louvet, S., Verlhac, M.H., Kubiak, J.Z., Maro, B., 1998. Cyclin synthesis controls the progression of meiotic maturation in mouse oocytes. *Development* 125, 4989–4997.
- Prodon, F., Chenevert, J., Sardet, C., 2006. Establishment of animal–vegetal polarity during maturation in ascidian oocytes. *Dev. Biol.* 290, 297–311.
- Prodon, F., Sardet, C., Nishida, H., 2008. Cortical and cytoplasmic flows driven by actin microfilaments polarize the cortical ER-mRNA domain along the a–v axis in ascidian oocytes. *Dev. Biol.* 313, 682–699.
- Sardet, C., Paix, A., Prodon, F., Dru, P., Chenevert, J., 2007. From oocyte to 16-cell stage: cytoplasmic and cortical reorganizations that pattern the ascidian embryo. *Dev. Dyn.* 236, 1716–1731.
- Savage, R.M., Danilchik, M.V., 1993. Dynamics of germ plasm localization and its inhibition by ultraviolet irradiation in early cleavage *Xenopus* embryos. *Dev. Biol.* 157, 371–382.
- Schneider, S., Steinbeisser, H., Warga, R.M., Hausen, P., 1996. Beta-catenin translocation into nuclei demarcates the dorsalizing centers in frog and fish embryos. *Mech. Dev.* 57, 191–198.
- Shimizu, T., 1999. Cytoskeletal mechanisms of ooplasmic segregation in annelid eggs. *Int. J. Dev. Biol.* 43, 11–18.
- Steinhauer, J., Kalderon, D., 2006. Microtubule polarity and axis formation in the *Drosophila* oocyte. *Dev. Dyn.* 235, 1455–1468.
- Takeda, N., Kyoizuka, K., Deguchi, R., 2006. Increase in intracellular cAMP is a prerequisite signal for initiation of physiological oocyte meiotic maturation in the hydrozoan *Cyrtis uchidae*. *Dev. Biol.* 298, 248–258.
- Teissier, G., 1931. Etude expérimentale du développement de quelques hydres. *Ann. Sci. Nat. Ser. X* 14, 5–60.
- van Eeden, F., St Johnston, D., 1999. The polarisation of the anterior–posterior and dorsal–ventral axes during *Drosophila* oogenesis. *Curr. Opin. Genet. Dev.* 9, 396–404.
- Wikramanayake, A.H., Huang, L., Klein, W.H., 1998. beta-Catenin is essential for patterning the maternally specified animal–vegetal axis in the sea urchin embryo. *Proc. Natl. Acad. Sci. U. S. A.* 95, 9343–9348.
- Wikramanayake, A.H., Hong, M., Lee, P.N., Pang, K., Byrum, C.A., Bince, J.M., Xu, R., Martindale, M.Q., 2003. An ancient role for nuclear beta-catenin in the evolution of axial polarity and germ layer segregation. *Nature* 426, 446–450.
- Zimyanin, V., Lowe, N., St Johnston, D., 2007. An oskar-dependent positive feedback loop maintains the polarity of the *Drosophila* oocyte. *Curr. Biol.* 17, 353–359.